Draft version September 20, 2022
Typeset using LaTeX default style in AASTeX631

Inference of Cosmological Parameters from WMAP Satellite CMB Data

Ingrid Gendron,[1] Noah LeFrancois,[1] and Katherine Savard[1]

[1] *Department of Physics, McGill University*
3600 Rue Universite,
Montreal, QC, H3A 2T8, Canada

ABSTRACT

Measurements of Cosmic Microwave Background (CMB) radiation by the Wilkinson Microwave Anisotropy Probe (WMAP) and Type Ia supernovae from the Supernova Cosmology Project Union Compilation can each be used to constrain cosmological parameters such as the Hubble parameter H_0, the spatial curvature of our universe Ω_k, and the fraction of our universe's total energy density accounted for by dark energy Ω_Λ and baryonic matter Ω_m. Using an ensemble Markov Chain Monte Carlo (MCMC) sampler, posterior probability distributions for these parameters are inferred from each data set. These distributions are then combined to provide an improved constraint upon the cosmological parameters which can be compared to the results of later surveys such as the Planck satellite. For the SNe Ia data the maximum likelihood values are found to be $H_0 = 69.98^{+0.43}_{-0.43}\frac{km/s}{Mpc}$, $\Omega_m = 0.28^{+0.07}_{-0.07}$, $\Omega_\Lambda = 0.72^{+0.11}_{-0.12}$ and $\Omega_k = 0.01^{+0.18}_{-0.18}$ which is in agreement with the surveys. For WMAP the values are $H_0 = 75.64^{+28.10}_{-25.50}\frac{km/s}{Mpc}$, $\Omega_m = 0.23^{+0.31}_{-0.11}$, $\Omega_\Lambda = 0.75^{+0.09}_{-0.24}$ and $\Omega_k = 0.01^{+0.02}_{-0.07}$ where the cosmological parameters are in agreement with the surveys however our value for H_0 is not. A correlated errors model for the CMB fit was also implemented in order to investigate the correlation strength present in the data. Due to limited computing resources and high run-time a comparison of results from this model to those of the uncorrelated error model was not completed, but could be investigated in future work.

Keywords: Markov Chain Monte Carlo — Cosmic Microwave Background — Type Ia Supernovae — Lamba-CDM Model

1. INTRODUCTION

The origin and evolution of our universe is a puzzle that astronomers and philosophers alike have studied for centuries. Arguably the most significant modern advancement in our understanding of this puzzle was the discovery of the Cosmic Microwave Background (CMB) Radiation, which not only ruled out the contested Steady-State theory of the universe, but was consistent with Big Bang cosmology described the Friedmann equations (derived from the expanding-universe solution to Einstein's general relativity field equations). The CMB offers a wealth of information about the beginnings of our universe, and the data can be used directly to derive parameters which describe it's composition and geometry.

The Wilkinson Microwave Anisotropy Probe (WMAP) is a spacecraft launched in 2001 which surveyed the CMB temperature anisotropy, playing a crucial role in establishing the current accepted model of cosmology, ΛCDM. The model was fitted to the measured temperature anisotropy using a powerful Markov Chain Monte Carlo (MCMC) algorithm (1) to obtain cosmological parameters that describe our universe such as the Hubble constant(H_0), the curvature of the universe(Ω_k), the dark energy density(Ω_Λ), and the cold dark matter density (Ω_c).

In our investigation, we recover these ΛCDM cosmological parameters from WMAP data by employing an MCMC algorithm in tandem with a ΛCDM interpolated model known as *PICO* (11) (a likelihood model interpolated from the true ΛCDM, and less computationally expensive than that used in the original WMAP analysis). In order to further constrain the posteriors recovered, we also include the analysis of Type Ia Supernovae (SNe). These are standardizable candles apparent at a multitude of redshifts and thus allow us to measure luminosity distance as a function of redshift, and therefore infer cosmological parameters.

This investigation will be organized as follows. We begin first by introducing the relevant theory in Section 2, describing both the physics related to the data (CMB Section 2.1, and Type Ia Supernovae Section 2.2) and model (ΛCDM Section 2.3), as well as the theory behind the tools we use to evaluate the model (Markov Chain Monte Carlo 3.1). In Section 3 we describe in detail the methods used to carry out the data analysis, as well as methods used to test the performance of our analysis. Finally, in Sections 4 and 5 respectively, we present and discuss our findings. Conclusions from these findings are summarized in Section 6.

2. THEORY

2.1. *Cosmic Microwave Background*

In the Big Bang theory of the origin of the universe, the mean density increases monotonically as one goes back in time. Under this assumption, the density at some early enough time must have been so great that baryonic matter and radiation were in thermodynamic equilibrium, and all atoms were ionized. In this time period, the mean free path of photons was small, and opacity was sourced by electron scattering – the universe was like a fog where photons could not escape. Not only was this state dense, but also very hot and characterized by a Planck spectrum. At approximately 380,000 years post Big Bang, a time known as "recombinations", the temperature of the universe had cooled enough that few of the photons were able to ionize hydrogen and therefore electrons and protons recombined and photons were freed from the main source of opacity. A this moment, at 3000K, the proverbial fog had lifted and the universe became transparent.

Once freed, these trapped photons then underwent negligible absorption or scattering and continue to propagate through the universe to this day, now observed as the CMB and originating from what is known as the 'surface of last scattering'. Since their original emission, these photons have been cosmologically redshifted to much lower wavelength (microwave) and their energy distribution forms a Planck spectrum at 3 degrees Kelvin. This characteristic temperature was predicted and accurately measured by WMAP data.

Data taken by WMAP is in the form of an angular power spectrum, a measurement of the temperature anisotropy as a function of multipole moment (angular frequency on the sky, inverse of angular scale). Tiny fluctuations in the primordial soup of particles at the beginning of the universe have been imprinted into the small-scale temperature fluctuation in the CMB, and so measuring these temperature fluctuations, and more specifically acoustic peaks ringing through the CMB, allow us to measure the angular diameter distance to recombination, the curvature of the universe, as well as baryon and dark matter density in the universe. In our investigation, we fit the WMAP power spectrum to a ΛCDM model of the universe to extract these parameters.

2.2. *Type Ia Supernovae*

Type Ia SNe are events which occur when a white dwarf is accreting matter from a companion star in a binary system, and the white dwarf exceeds a critical mass (known as the Chandrasekhar mass) igniting nuclear fusion, causing a subsequent runaway reaction and therefore a supernova explosion. Due to the fixed critical mass of the white dwarf, the peak luminosity of this type of explosion is extremely consistent and can be used as a standard candle for distance measurements. Luminosity distance as a function of redshift is dependent on cosmological parameters, and so SNe luminosity data at various redshifts can be used to constrain cosmological models.

The Supernova Cosmology Project Union 2.1 Compilation(2) concatenates the luminosity of Type Ia SNe at a range of redshifts from various surveys, providing a rich source of data for us to fit to the ΛCDM model and further constrain the cosmological parameters obtained from WMAP data.

2.3. *ΛCDM Cosmological Model*

ΛCDM might be one of the simplest models that explains the properties of the cosmos, nevertheless it is the most supported model by astronomers and astrophysicists. The name of the model refers to the three components which the universe contains: dark energy (Λ), cold dark matter (CDM) and ordinary matter. The properties of the cosmos are listed as: the existence and structure of the cosmic microwave background, large-scale structure in the distribution of galaxies and the accelerating expansion of the universe observed in the light from distant galaxies and supernovae. It is therefore applicable to many data sets like the type SNe Ia and WMAP mentioned above in order to infer the density parameters that describe the universe we live in.

As seen in Lab 2 of the course, the derivation of the expansion of the universe using the Friedman equations leads to a relationship between the various density parameters $1 = \Omega_m + \Omega_r + \Omega_\Lambda + \Omega_k$ where the matter density is Ω_m,

radiation density Ω_r, dark energy density Ω_Λ and the curvature of the universe Ω_k. However, (3) show that the radiation density is approximately 10^{-5} and it can be neglected from the equation resulting in

$$1 = \Omega_m + \Omega_\Lambda + \Omega_k \tag{1}$$

Ω_m is the combination of dark matter density Ω_c and baryon density parameter Ω_b which is described as

$$\Omega_m = \Omega_c + \Omega_b \tag{2}$$

It is atypical for these cosmological parameters to be solved for in this form, however, and result papers (2)(4) (5) (6) solve for the **physical** baryon density ($\Omega_b\, h^2$) and **physical** dark matter density($\Omega_c\, h^2$) parameters, where h is defined as:

$$h = \frac{H_0}{100}\frac{km/s}{Mpc}. \tag{3}$$

2.4. *Markov Chain Monte Carlo*

The Markov Chain Mont Carlo (MCMC) algorithm is a simple yet powerful computational tool for performing Bayesian inference, and has been widely used in cosmology and astrophysics in recent years (7)(8). This algorithm is based on a random walk in the parameter space of the likelihood function using rejection sampling, where the proposed next step is randomly generated and then accepted or rejected with some acceptance probability based on the relative likelihoods of the current state and the proposed state. The acceptance probability is lower for less likely proposed states, and higher for highly likely proposed states. If the proposed state is more likely than the current state, the step is always accepted and added to the "chain", or list of steps along the random walk. As a result, for a sufficiently large number of steps the distribution of samples in the chain will converge to the posterior probability distribution of the model given a set of data. (9)

The *emcee* package implements an MCMC algorithm in *Python* (7), which can be easily deployed for Bayesian inference in high-dimensional parameter spaces. For a d-dimensional model, *emcee* needs to be supplied with a function to evaluate the likelihood probability function of interest given a vector of parameters $\theta = (\theta_1, \cdots, \theta_d)$. In Section 3 of this paper, we will outline the methods used to apply MCMC fitting models to CMB and SNe Ia data, including the definition of likelihood probability functions for each model. We will also discuss how we check that a chain is converged and how we obtain a posterior probability distribution containing independent samples from the chain.

3. METHODS

3.1. *MCMC Parameter Fitting*

3.1.1. *Cosmic Microwave Background*

The CMB power spectrum can be computed as a function of the cosmological parameters introduced in Section 2.3 by a number of *Python* libraries. Code for Anisotropies in the Microwave Background (*CAMB*) (10) is one such library which can accurately perform these calculations, however it has a high computational cost which is a serious drawback due to the large number of function calls used by an MCMC.

Parameters for the Impatient Cosmologist (*PICO*) (11) achieves a speed improvement of 2 orders of magnitude by fitting an interpolating function to training data obtained from *CAMB*. Due to our limited computing resources and time constraints, we utilized *PICO* for our CMB fitting.

A uniform prior for the CMB posterior probability was chosen:

$$log(P_{prior}(\theta)) = \begin{cases} 0 & 0 \leq \Omega_b \leq 1, 0 \leq \Omega_c \leq 1 \\ -\infty & |i-j| = 1 \end{cases} \tag{4}$$

Ω_b and Ω_c were constrained to be between 0 and 1 since they are density fractions, and are therefore normalized quantities. We chose a uniform prior in order to minimize the bias we introduce into the analysis. Our goal is to verify whether we reproduce similar posterior probability distributions to those in the publications discussed in Section 5, and as a result we don't want to introduce a biased prior probability distribution informed by our knowledge of those results.

In order to evaluate the CMB likelihood probability we use the χ^2 metric for evaluating the fit of a model to data:

$$\chi^2 = \sum (\frac{y_{d,i} - y_{m,i}}{\sigma_i})^2 \tag{5}$$

where $y_{d,i}$ is the value of data point i and $y_{m,i}$ is the value of the model evaluated at the location of point i.(12) The χ^2 measures the deviation of the observed data from the model's fit, weighted inversely by the uncertainties in the individual points. The likelihood function for a model with parameters θ can be written in terms of χ^2 as:

$$P_{likelihood}(\theta) \propto e^{-\chi^2} \tag{6}$$

and therefore the log-likelihood probability is simply equal to χ^2.(13)

This metric assumes that the data contains Gaussian noise which is uncorrelated between data points, i.e. the noise at point i is an independent process from the noise at any other point $j \neq i$. Eq. 5 is the special case of Eq. 7 where the covariance matrix, $\mathbf{C}$, is an identity matrix and therefore contains no correlation:

$$\chi^2 = (y_d - y_m)^T \mathbf{C}^{-1} (y_d - y_m) \tag{7}$$

While this is often a reasonable approximation, in some cases where there is strong correlation between data points this metric can underestimate the width of our confidence intervals.(12)

We can loosen the constraint with a model for Gaussian noise which has correlation between adjacent data points. This model would produce a covariance matrix which is is zero outside of the diagonals $i = j$, $i = j + 1$, and $i = j - 1$ (**?**):

$$C_{ij} = \begin{cases} \sigma_i^2 & i = j \\ \alpha |\sigma_i \sigma_j| & |i - j| = 1 \\ 0 & |i - j| > 1 \end{cases} \tag{8}$$

The scaling parameter α varies from -1 to 1, and controls the strength of the correlation between adjacent points. These bounds on the value of α is added as an additional constraint on the prior. By leaving α as a floating parameter in our likelihood function, we can fit for the correlation strength in our MCMC chain alongside the *PICO* model parameters.

The log-posterior probability function is then equal to the sum of the log-prior and log-likelihood probability functions; it will have a value of $-\infty$ if θ lies outside of our uniform prior region, else it will simply be equal to the log-likelihood probability.

3.1.2. *Type Ia Supernovae*

The distance modulus $m - M$ was computed as a function of redshift according to Eq. 9, where D_L is the luminosity distance at which the supernova occurs. D_L is calculated by the *astropy* library using a *LambdaCDM* model with the cosmological parameters H_0, Ω_m, and Ω_Λ .

$$m - M = 5 log_{10}(D_L) + 25 \tag{9}$$

The SNe Ia likelihood probability was calculated using the uncorrelated χ^2 metric given by Eq. 5.

A uniform prior for the SNe Ia posterior probability was chosen:

$$log(P_{prior}(\theta)) = \begin{cases} 0 & 0 \leq \Omega_m \leq 1, 0 \leq \Omega_\Lambda \leq 1 \\ -\infty & |i - j| = 1 \end{cases} \tag{10}$$

Ω_m and Ω_Λ were constrained to be between 0 and 1 since they are density fractions, and are therefore normalized quantities. As was the case for the WMAP data, we chose a uniform prior in order to minimize the bias we introduce into the analysis.

As was the case for the CMB fitting, the log-posterior probability function is then equal to the sum of the log-prior and log-likelihood probability functions.

3.2. *Convergence Monitoring*

Determining the convergence of an MCMC is deemed to be somewhat of a heuristic and qualitative process, but there exist steps one can take to ensure convergence is at least likely. One common way of determining convergence is through the use of the integrated autocorrelation time τ, which is the average number of steps a walker needs to 'forget' an initial starting point in parameter space, and $\frac{N}{\tau}$ is the effective number of samples needed (for N samples). The integrated autocorrelation time can be estimated as the sum of "the normalized autocorrelation function of the stochastic process that generated the chain" (14), and in this investigation we offload this calculation to the *sampler.get_autocorr_time*() function in the *emcee* library (7). Once τ is calculated, a modest estimate of the required burn in time is commonly estimated as twice the maximum τ encountered, while the scale at which we thin our samples is estimates as half the minimum τ encountered.

We employ these metrics of determining convergence in our function to run the MCMC, given the switch "burn-in" to the function. With this switch activated, the function runs the MCMC for a arbitrarily large number of steps (100,000 in this case) and every 100 steps the autocorrelation time is recorded. For each autocorrelation time calculated, if the number of steps exceeds 100 times the estimated autocorrelation time and this estimate has changed by less than 1% compared to the previous check, we deem the chain converged and stop stepping.

For the WMAP data, we could not run the MCMC long enough to see convergence as described above, and we therefore ran the algorithm as long as reasonably possible and recorded our results. For the SNe data, we saw the MCMC converge and ran for an arbitrary number of steps after convergence to define our corner plot contours.

4. RESULTS

The SNe Ia data converged, resulting in a mean auto correlation time and burn-in length of 37.38 steps and 76 steps respectively, with a thinning factor of 18. The plot of SNe Ia data MCMC convergence can be found in Fig.1. However, the WMAP data was unable to converge within an appropriate length of time and we decided that out of 100,000 iterations a burn in of 2000 and a thinning of 20 was appropriate (justified in Section 5).

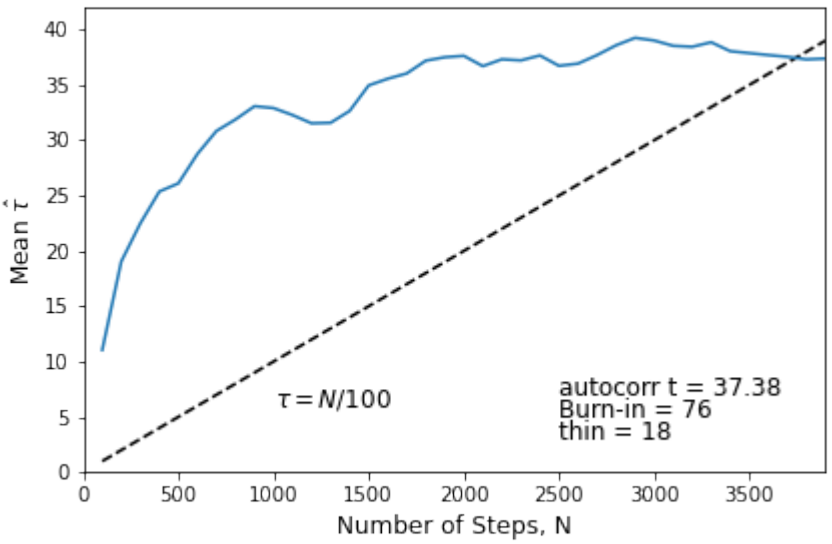

Figure 1. Convergence of the SNe Ia MCMC chains. τ represents the number of steps that are needed before the chain forgets where it started. The dotted black line represents $\frac{N}{100}$ where any τ before this line should not be trusted. The auto correlation time is found to be 37.38, the burn-in is 76 steps and the thinning 18 factor.

The corner plots for SNe Ia can be found in Fig.2 with the variable posterior distributions for H_0, Ω_m, Ω_Λ. The maximum likelihood value solved for in the MCMC are $H_0 = 69.97^{+0.44}_{-0.44}$, $\Omega_m = 0.28^{+0.07}_{-0.07}$ and $\Omega_\Lambda = 0.72^{+0.11}_{-0.12}$. Rearranging Eq.1 then it is possible to solve for curvature $\Omega_k = 0.01^{+0.19}_{-0.18}$.

Fig.3 displays the corner plots for the WMAP data with the maximum likelihood values given for $H_0 = 75.64^{+28.10}_{-25.50}\frac{km/s}{Mpc}$, $\Omega_b\,h^2 = 0.02^{+0.00}_{-0.00}$, $\Omega_c\,h^2 = 0.11^{+0.01}_{-0.00}$ and $\Omega_k = 0.01^{+0.02}_{-0.07}$. Using Eq.3 we can solve for h at each

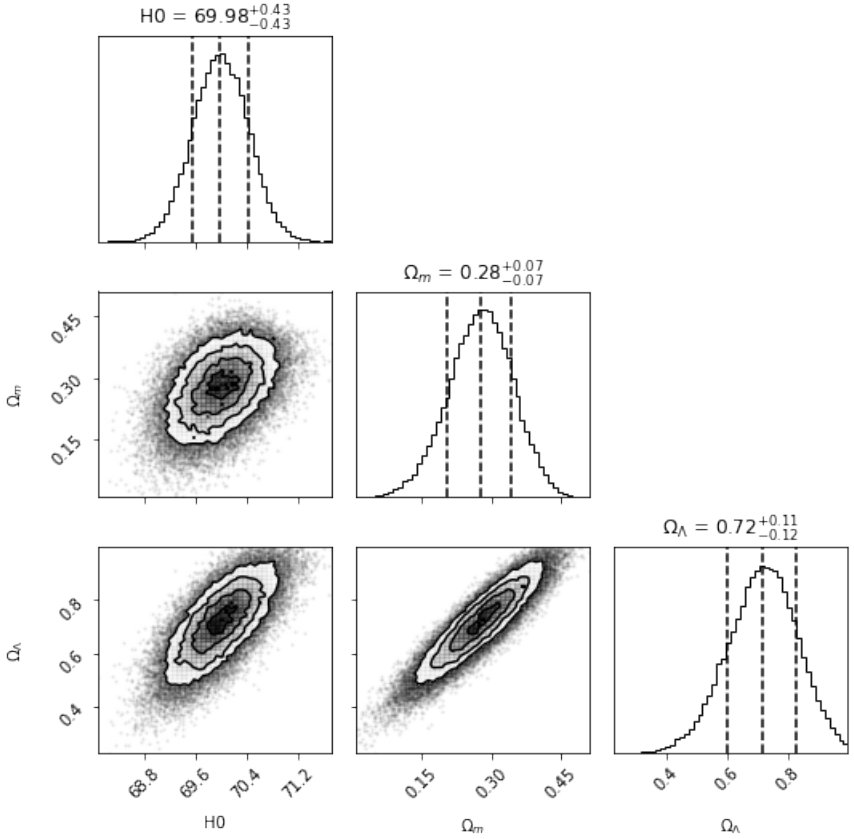

Figure 2. SNe corner plot representing the maximum likelihood value and confidence interval for H_0, Ω_m and Ω_Λ. Computing the SNe Ia data using *LambdaCDM* from *astropy* we find that $H_0 = 69.98^{+0.43}_{-0.43}\,\frac{km/s}{Mpc}$, $\Omega_m = 0.28^{+0.07}_{-0.07}$, $\Omega_\Lambda = 0.72^{+0.11}_{-0.12}$ and using Eq.1 to solve for curvature $\Omega_k = 0.01^{+0.18}_{-0.18}$.

step of the MCMC chain and calculate a new likelihood probability for Ω_m. Eq.2 is used to calculate $\Omega_m = 0.23^{+0.31}_{-0.11}$. Knowing Ω_m and Ω_k rearranging Eq.1 to solve for $\Omega_\Lambda = 0.75^{+0.09}_{-0.24}$.

To make sure the MCMC is solving for reasonable cosmological parameters, we plot in Fig 4 A) the raw SNe Ia data as well as the MCMC fits of the *LambdaCDM* model. As the MCMC has a high number of iterations, only the last 100 *LambdaCDM* fits are plotted. An animation of the fits in order of occurrence in the MCMC can be seen at SNe_MCMC_uncorr_animation.gif. The fit qualitatively seems to adequately describe the data, allowing us to assume the MCMC was performing well and sampling a suitable range of parameter space.

Fig 4 B) displays the WMAP data as well as the CMB power spectra fit from *PICO* for the last 100 samples of the MCMC excluding the burn-in. An animation of the fits in order of occurrence in the MCMC can be seen at WMAP_MCMC_uncorr_animation.gif. Here as well it can be argued that the fit is qualitatively sufficient in describing the WMAP data.

Combining the posterior fits for Ω_Λ as a function of Ω_m, which can be seen in Fig. 5, from the SNe and WMAP data we can recreate the plot from (4), minus the additional constraints also considered in the paper. For reference, the flat universe boundary is plotted alongside the posteriors. The intersection of the SNe and CMB models show that a flat universe is consistent with the data.

5. DISCUSSION

Firstly, we will discuss the results corresponding the the SNe data. According to previous studies of Type Ia SNe to determine cosmological parameters, N. Suzuki et al (4) and R. Amanullah et al (2), they found values of $\Omega_m = 0.277^{+0.022}_{-0.021}$ and $\Omega_\Lambda = 0.729^{+0.014}_{-0.014}$, using a measured value for H_0 to constrain Ω_Λ. They used a value of $H_0 = 74.8 \pm 3.1\frac{km/s}{Mpc}$ and assume a flat universe ($\Omega_k = 0$). We want to verify how well our fit using *astropy*

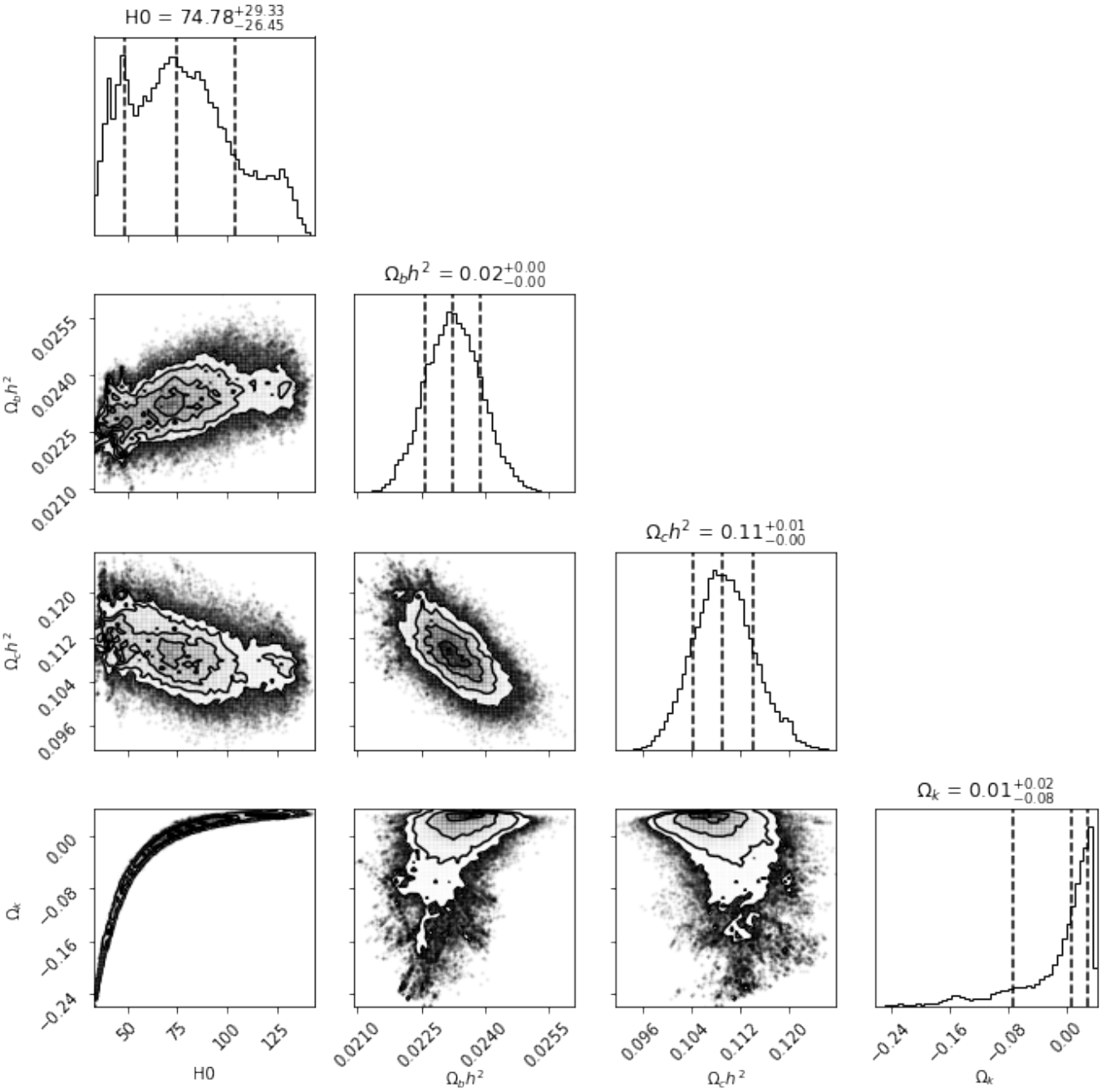

Figure 3. CMB corner plot representing the maximum likelihood value and confidence interval for H_0, $\Omega_b\,h^2$, $\Omega_c\,h^2$, Ω_Λ and Ω_k. Computing the CMB data using *PICO* the parameters are found to be $H_0 = 75.64^{+28.10}_{-25.50}\frac{km/s}{Mpc}$, $\Omega_b\,h^2 = 0.02^{+0.00}_{-0.00}$, $\Omega_c\,h^2 = 0.11^{+0.01}_{-0.00}$ and $\Omega_k = 0.01^{+0.02}_{-0.07}$. Using Eq.3 we can find h then from there use Eq.2 to find $\Omega_m = 0.23^{+0.31}_{-0.11}$. To get Ω_Λ, using Eq.1 knowing Ω_m and Ω_k which can solve for $\Omega_\Lambda = 0.75^{+0.09}_{-0.24}$.

LambdaCDM compares to (4) and (2). Our values are within the confidence interval for Ω_m and Ω_Λ. We did not use a *FlatLambdaCDM* model (another option in the *astropy* library which assumed zero curvature) but inferred Ω_k using Eq. 1 where we find that the curvature is $\Omega_k = 0.01^{+0.18}_{-0.18}$ which is consistent with a flat universe. However, our value of $H_0 = 69.98^{+0.43}_{-0.43}\frac{km/s}{Mpc}$ is not within the confidence interval to the measured value (4) and (2) used. Even comparing to the Planck data (5) the value found for $H_0 = (67.8 \pm 0.9)\frac{km/s}{Mpc}$ is not within the confidence interval. Looking at

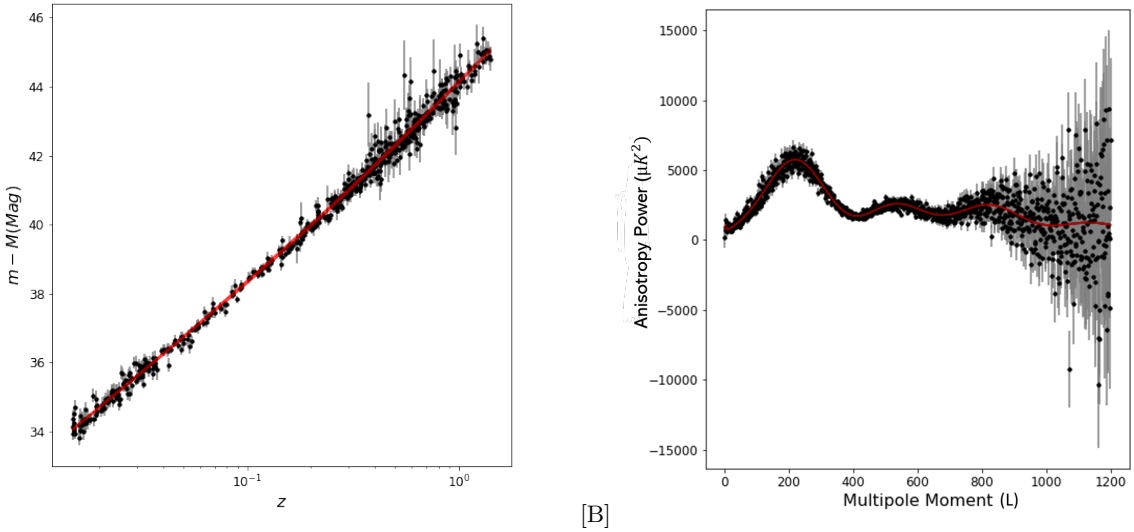

[A] [B]

Figure 4. A) SNe data points with given error bars plotted with the posterior fits computed with *astropy LambdaCDM*. The data points are in black with their corresponding grey error bars. The line in red represents to overlayed fits of the *LambdaCDM* parameters calculated from the last 100 steps of the MCMC. B) WMAP data points with given error bars plotted with the posterior fits computed with *PICO*. The data points are in black with their corresponding grey error bars. The line in red represents to overlaid fits of the power spectra calculated from the last 100 steps of the MCMC. An animation of the fits can be seen in SNe_MCMC_uncorr_animation.gif and WMAP_MCMC_uncorr_animation.gif respectively.

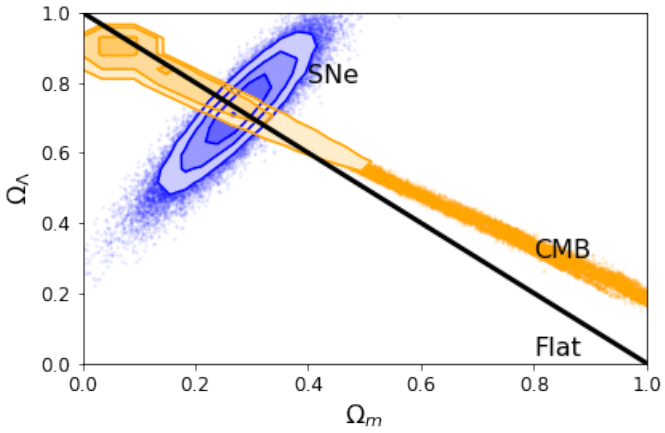

Figure 5. SNe and CMB posterior fits for dark energy density as a function of matter density parameters. The orange posterior represents the CMB data computed by *PICO*. The blue posterior represents the SNe data computed by *LambdaCDM* function from *astropy*. The black line represents the flat universe where Ω_k equals zero. The darker the color, the more dense the likelihood.

the fits to the SNe Ia data in Fig.4 the model computed by *LambdaCDM* qulitatively describes the data well. The posterior probability functions in Fig. 2 A) for each parameter display Gaussian-like distributions clearly peaked at a single value. To conclude, The *LambdaCDM* function in *astropy* is a quick way and precise way to fit SNe Ia data to get reasonable results.

As for the WMAP data, we were unable to see the MCMC to convergence due to time constraints, and therefore we were also unable to determine the burn-in and thinning. The MCMC code itself was not the problem as the SNe Ia data converged rapidly. Our hypothesis, after looking at the chain of values visited, is that convergence wasn't reached due to the H_0 parameter. We observed that a wide range of H_0 values were randomly explored, and no discernible peak likelihood was found. After running the MCMC for 48 hours, it stated that there was still not enough iterations to converge. Instead, from observing the walkers from a few independent MCMC runs for H_0 we decided that around

2000 steps was a convenient place to start, as this is where H_0 experienced the lowest amplitude oscillations in value at 70 $\pm 25 \frac{km/s}{Mpc}$.

Comparing our *PICO* fit parameters to G. Hinshaw et.al (6) where they use the 9 year WMAP data to fit $\Omega_b\, h^2$ and $\Omega_c\, h^2$ of the ΛCDM model, our results are in agreement. For $\Omega_b\, h^2$ they find a value of 0.02264±0.00050 where our *PICO* fit was found to be 0.02 ±0.00. For $\Omega_c\, h^2$ they fit for a value of 0.1138±0.0045 which is consistent with our value of $0.11^{+0.01}_{-0.01}$. The derived parameter Ω_Λ obtained from Eq.1 is $0.75^{+0.09}_{-0.24}$ where the lower bound is approximately 30% of the value itself raises some questions about how we bounded the parameters, and how accurate our results are. The same goes with $\Omega_m = 0.23^{+0.31}_{-0.11}$ where the upper bound is larger than the value itself. However, compared to (6) they found $\Omega_\Lambda = 0.721 \pm 0.025$ which is in agreement with our results. The problem here is our fitted value of H_0 is $74.78^{+29.33}_{-26.45} \frac{km/s}{Mpc}$. The problem could lie in the fact that the data used is outside of the training data of *PICO*. Even so, all the parameters visited by H_0 are physical and therefore we could not justify constraining it in the prior. To conclude, *PICO* is a much faster alternative to CMB model and still yields agreeable results, but only works when the parameter space that the solution lives in is within the training space. The main improvement would be to constrain H_0 further, as that seems to be the largest weakness. A solution is to use *CAMB* in regions of the parameter space that lie outside of the *PICO* training space, however this was out of the scope for our investigation.

Both *LambdaCDM* and *PICO* are useful python packages that make fitting the cosmological parameters to the ΛCDM model easy and result in acceptable fits.

We conclude our analysis by comparing fitted cosmological parameter values from both data sets those obtained from the Planck survey. We compare to the most constrained values, and find that all of our derived parameters are in agreement with Planck. To recap, all parameters for Ω_m, Ω_Λ and Ω_k can be seen in Table 1

	SNe Ia	WMAP	SNe Ia [(4) (2)]	WMAP [(6)]	Planck(Lowest constraint) [(5)]
Ω_m	$0.28^{+0.07}_{-0.07}$	$0.23^{+0.31}_{-0.11}$	$0.277^{+0.022}_{-0.021}$	$\sim$	0.315 ± 0.013
Ω_Λ	$0.72^{+0.11}_{-0.12}$	$0.75^{+0.09}_{-0.24}$	$0.729^{+0.014}_{-0.014}$	$0.721^{+0.025}_{-0.025}$	0.685 ± 0.013
Ω_k	$0.01^{+0.18}_{-0.18}$	$0.01^{+0.02}_{-0.07}$	0.0(fixed)	$-0.037^{+0.044}_{-0.042}$	<0.005

Table 1. Summary of the three cosmological parameters from the MCMC fit from *LambdaCDM* and *PICO*. There is also the referenced values from Planck (5) as well as Sne Ia (4) (2) and 9 year WMAP (6) accepted papers.

Finally, we recreated the constraint plot from R. Adam et.al (5) where they plotted the posteriors of Ω_Λ as a function of Ω_m for different sets of data: SNe Ia data, CMB data, CMB data combined with an addition phenomena, in order to gain insight on Ω_k which describes the shape of the universe. In Fig. 5 it's easy to see that the intersection of the SNe likelihood with the CMB likelihood encompasses part of the flat line. This flat line represents where a flat universe exists, in other words Ω_k is zero. From that we can conclude that our values are consistent with a flat model universe and the posteriors are similar in shape to R. Adam et.al (5). It would be an interesting extension to include the additional data that R. Adam et.al (5) included in their plot, that from the measurements of the Baryonic Acoustic Oscillations.

6. CONCLUSION

In this project we applied an ensemble MCMC technique to the problem of inferring the posterior probability distributions of a number of cosmological parameters. The Hubble constant, dark energy density fraction, matter density fraction, and curvature of our universe were constrained through the fitting of CMB data from the WMAP satellite as well as Type Ia supernovae data from the Supernova Cosmology Project Union Compilation. These inferred distributions were compared to the results obtained by various publications on the same problem, and our maximum likelihood values were found to be consistent in most cases. A notable exception was the Hubble constant inferred from our CMB analysis, as our probability distribution displayed an extremely large spread and no distinct Gaussian peak compared to the rest of our distributions as well as the literature values.

We investigated the convergence of our MCMC chains as well as the fraction of independent samples obtained; the SNe Ia chain converged efficiently but our CMB chain did not converge even after 1 million samples. Due to limited computing resources and time constraints, we were unable to investigate further. Similarly, a model for correlated errors in the CMB fit was implemented in order to infer the correlation strength of the data, but this approach also suffered from excessive computational cost and useful results were not obtained in the time-frame of this project.

Areas for future work include investigating the convergence of the CMB chain, the analysis of our CMB correlated errors model and the application of this technique to the SNe Ia data. Furthermore, a variety of different priors and constraints on inferred parameters of the MCMC were used in the literature sources we compared to. A deeper investigation of how these priors and constraints influence the probability distribution produced would improve our understanding of the results and provide a more direct comparison to measure our code performance by.

REFERENCES

[1]C.L. Bennett et.al., *Nine-Year Wilkinson Microwave Anisotropy Probe (WMAP) Observations: Final Maps and Results*, ApJS (2012)

[2]R. Amanullah et.al., *Spectra and Light Curves of Six Type Ia Supernovae at 0.511 < z <1.12 and the Union2 Compilation*, arXiv (2010)

[3]E.D. Valentino, A. Melchiorri, J. Silk, *Planck evidence for a closed Universe and a possible crisis for cosmology*, arXiv (2019)

[4]N. Suzuki et.al., *The Hubble Space Telescope Cluster Supernova Survey: V. Improving the Dark Energy Constraints Above z>1 and Building an Early-Type-Hosted Supernova Sample*, arXiv (2011)

[5]R. Adam et.al., *Planck 2015 results. I. Overview of products and scientific results*, arXiv (2015)

[6]G. Hinshaw et.al., *Nine-Year Wilkinson Microwave Anisotropy Probe (WMAP) Observations: Cosmological Parameter Results*, arXiv (2012)

[7]D. Foreman-Mackey, D.W. Hogg, D. Lang, J. Goodman, *emcee: The MCMC Hammer*, Publications of the Astronomical Society of the Pacific, Vol. 125, Issue 925, pp. 306 (2013)

[8]J. Akeret, S. Seehars, A. Amara, A. Refregier, A. Csillaghy *CosmoHammer: Cosmological parameter estimation with the MCMC Hammer*, arXiv (2012)

[9]N. Christensen, R. Meyer, L. Knox, B. Luey, *Bayesian Methods for Cosmological Parameter Estimation from Cosmic Microwave Background Measurements*, arXiv (2001)

[10]A. Lewis, A. Challinor, *CAMB: Code for Anisotropies in the Microwave Background*, J. Astrophysics Source Code Library (2011)

[11]W. A. Fendt, B.D. Wandelt, *PICO: Parameters for the Impatient Cosmologist*, The Astrophysical Journal, Vol. 654, pp. 2-11 (2007)

[12]B. Montet, *Beyond Chi-Squared: An Introduction to Correlated Noise*, Astrobites. Web. Published Jul 1, 2014. Accessed Apr 11, 2021

[13]J. Conway, *Data Modelling and Fitting*, CDF Statistics Committee. Web. Published Sept 2002. Accessed Apr 11, 2021

[14]D. Foreman-Mackey et al.(2012-2019) *Autocorrelation analysis convergence.* emcee. https://emcee.readthedocs.io/en/stable/tutorials/autocorr/

[15]D. Foreman-Mackey, *corner.py: Scatterplot matrices in Python*, The Journal of Open Source Software, Vol. 1, No. 2, pp. 24 (2016)